Dyes and Pigments 224 (2024) 112042

Contents lists available at ScienceDirect

Dyes and Pigments

journal homepage: www.elsevier.com/locate/dyepig

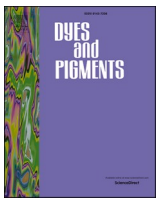

Optical evaluation of dansyl derivatives and their implementation in low-cost and flexible dye-doped PMMA platforms for efficient detection of hazardous chemical vapours

Gonçalo Pedro [a], Frederico Duarte [a], Georgi M. Dobrikov [b,**], Atanas Kurutos [b,c], Hugo M. Santos [a,d], José Luis Capelo-Martínez [a,d], Elisabete Oliveira [a,d,***], Carlos Lodeiro [a,d,*]

[a] BIOSCOPE Research Group, LAQV-REQUIMTE, Chemistry Department, NOVA School of Science and Technology, FCT NOVA, Universidade NOVA de Lisboa, 2829-516, Caparica, Portugal
[b] Institute of Organic Chemistry with Centre of Phytochemistry, Bulgarian Academy of Sciences, Acad. G. Bonchev str., bl. 9, 1113, Sofia, Bulgaria
[c] University of Chemical Technology and Metallurgy, 8 St. Kliment Ohridski blvd, 1756, Sofia, Bulgaria
[d] PROTEOMASS Scientific Society, Praçeta Jeronimo Dias, 12-2A, 2825-466, Costa de Caparica, Portugal

ARTICLE INFO

Keywords:
Dansyl derivatives
Fluorescent chemosensors
Dye-doped PMMA polymers
Solvatochromic properties
Acidic vapours detection

ABSTRACT

This work investigates the creation and analysis of six novel dansyl derivatives (named **L1** to **L6**) and their incorporation into PMMA polymers for environmental sensing purposes. The properties of these derivatives were extensively examined in different solvents and solid states. Notably, they exhibited a significant change in color depending on the solvent's polarity, suggesting their potential to assess microenvironmental polarity. Moreover, these derivatives showed promising capabilities in selectively detecting Cu^{2+} and Hg^{2+} metal ions in acetonitrile solution, forming individual species with these metals. Furthermore, their responsiveness to changes in acidity and basicity was explored both in acetonitrile solution and within a PMMA polymer matrix, indicating their potential for pH-sensitive applications. By integrating these derivatives into PMMA polymers, acid-base sensitive materials were produced, suitable for monitoring environmental conditions such as hazardous gas detection and pH level changes. This integration addresses the solubility challenges of dansyl compounds and broadens their use in various sensing applications.

1. Introduction

In recent years, there has been considerable attention directed towards the development of fluorescent chemosensors, primarily because of their exceptional sensitivity, speed, and non-invasive nature in analytical processes [1,2]. One of the commonly used fluorophores in this field is the dansyl group, which offers several advantages; it exhibits emission in the visible region, possesses an exceptionally high fluorescence quantum yield, and exhibits a significant Stokes shift, thereby avoiding any auto-absorption effects. These compounds incorporated electron-donating and electron-withdrawing moieties, which contribute to their high fluorescence quantum yields [3,4]. Furthermore, the fluorescence intensity and emission maximum of dansyl-based compounds are known to vary with the polarity of the surrounding environment, primarily due to their charge transfer properties being very useful for biological applications [5–8]. Based on the reports published in the literature [1,9,10], dansyl derivatives have demonstrated selective detection capabilities for Cu^{2+} and Hg^{2+} metal ions, as well as certain anions. These favourable properties make them highly relevant in fields such as environmental monitoring, bioanalytical chemistry, and clinical diagnostics. The advantage of dansyl-based compounds lies in their ability to provide tailored selectivity, allowing for precise and reliable detection of these target analytes even in complex matrices. Considering the ongoing pursuit for metal ion sensing systems, our

* Corresponding author. BIOSCOPE Research Group, LAQV-REQUIMTE, Chemistry Department, NOVA School of Science and Technology, FCT NOVA, Universidade NOVA de Lisboa, 2829-516, Caparica, Portugal.
** Corresponding author.
*** Corresponding author. BIOSCOPE Research Group, LAQV-REQUIMTE, Chemistry Department, NOVA School of Science and Technology, FCT NOVA, Universidade NOVA de Lisboa, 2829-516, Caparica, Portugal.
E-mail addresses: Georgi.Dobrikov@orgchm.bas.bg (G.M. Dobrikov), ej.oliveira@fct.unl.pt (E. Oliveira), cle@fct.unl.pt (C. Lodeiro).

https://doi.org/10.1016/j.dyepig.2024.112042
Received 31 December 2023; Received in revised form 18 February 2024; Accepted 18 February 2024
Available online 19 February 2024

group reported two novel dansyl derivatives that exhibited modifications in their photophysical properties in the presence of Cu^{2+} and Hg^{2+}, where the presence of heteroatoms in the structure was deemed crucial for the sensing mechanism. These compounds displayed an LOD and LOQ of 2.5 μM and 4.5 μM, respectively, towards Hg^{2+} ions and exhibited a solvatochromic behaviour which was modulated in the presence of water, resulting in a fluorescence enhancement via aggregation-induced emission, exemplifying the multiple properties of dansyl derivatives [7]. Similarly, Ming Zhou et al. synthesized a dansyl-based chemosensor that exhibited remarkable fluorescence quenching upon the addition of Cu^{2+} over other metal ions. This sensitivity was attributed to the complex formation with a 6.7×10^5 M^{-1} association constant, achieving a detection limit (LOD) of 0.25 μM. Additionally, this detection was carried out in a pH range of 5.0–14.0, as well as used in detecting Cu^{2+} in living cells, illustrating the potential for biological applications for dansyls [11]. Using a peptide-based dansyl derivative, Yongxin Li and colleagues managed to detect several mercury species by the coordination of mercury ions and organic mercury to the peptide sequence. The authors reported a rare system with different responses for Hg^{2+} ions (fluorescence turn-off response) and organic mercury (turn-on response), without interference from other substances. For Hg^{2+} ions, the authors reached LOD values of 40 nM, providing new, sensitive and selective approaches for mercury monitoring [12].

However, it is worth noting that one restriction of dansyl derivatives is their limited solubility in water, which can hinder their application in biological and environmental contexts where aqueous environments are prevalent. The hydrophobic nature of these compounds restricts their dispersion and interaction with aqueous samples, thereby limiting their effectiveness as probes in such settings. To overcome this limitation and expand the applicability of dansyl based compounds in biological and environmental applications, researchers have explored various strategies. One such strategy is namely the incorporation of dansyl derivatives into polymers. This approach involves the synthesis or modification of polymers to include dansyl groups, thereby improving the solubility and dispersibility of the compounds in aqueous media. The incorporation of dansyl derivatives into polymers offers multiple advantages and applications. Firstly, it provides a solid platform for immobilizing the probes, allowing for easy handling and practical use. The solid state nature of polymer based systems also enhances stability, which is essential for long-term sensing applications. Additionally, polymers can be tailored to have specific properties such as biocompatibility or environmental resistance, further expanding the range of applications for dansyl based probes. [13].

Thus, by incorporating dansyl derivatives into polymers, researchers can overcome the solubility limitation and create a robust sensing platform that retains their selective detection properties. This strategy not only improves the practicality of these compounds but also enables their use in various biological and environmental sensing applications, where stability, ease of use, and compatibility with different media are crucial considerations.

A thorough examination of the available literature reveals that polymers, alongside other materials, have also emerged as key materials in various gas sensor devices offering a promising and cost effective solution for addressing issues related to hazardous gases in the environment. Conducting polymers has demonstrated remarkable applications in sensing gases with acid-base or oxidizing characteristics. Furthermore, when combined with other polymers like PVC and PMMA, which possess active functional groups capable of detecting such gases, they have shown significant potential [14–16]. Legislative measures have encouraged a substantial demand for sensors used in environmental monitoring, such as the detection of toxic gases and vapours in work places and contaminants in natural waters originating from industrial effluents and agricultural runoff. Literature has also documented the utilization of polymer films to create on-off systems for acid-base sensing. Recently, P. Gayathri et al. synthesized a triphenylamine-based fluorophore and inserted it in a PMMA polymer matrix. The systems exhibited turn-off fluorescence upon immersion in hydrazine (5%), followed by turn-on fluorescence by immersing in acetic acid (5%), achieving a 0.021% concentration limit of detection for hydrazine [17]. Raquel Jiménez et al. developed a similar system using a difluoride boron derivative and upon undergoing acid immersion studies observed that there were color changes at naked eye, accompanied by a red-shift in emission spectra, in response to highly acidic media. These results were attributed to the protonation of a pyridine group, leading to alterations in the optical properties and demonstrate the potential for industrial applications in detection of superacids [18]. Fu-Qiang Song et al. doped PMMA matrixes with salicylacylhydrazone Zn and Cd complexes and obtained interesting results. The system was shown to have a linear relationship between the fluorescence quenching efficiency and the concentration of picric acid in concentrations as low as 25 μM. The doped polymer film exhibited LOD and LOQ of 4.83 μM and 3.35 μM respectively, which were around 50% lower than the results for liquid state [19]. Moreover, some authors have reported doped polymer systems capable of detecting metals in solution, presenting new opportunities for the detection of metal ions [16,20,21].

Here in this study, a series of six new dansyl derivatives (**L1** to **L6**) were synthesized and thoroughly characterized. The photophysical properties of all compounds were investigated in various solvents, including DMSO, CH_3CN, ethanol, THF, and $CHCl_3$. To comprehensively explore the diverse characteristics of these compounds, they were primarily investigated for their solution based properties, particularly the ability to sense metal ions. Additionally, these compounds were incorporated into PMMA polymers as sensing elements to detect acidic and basic environmental conditions on solid supports.

2. Experimental section

2.1. Materials and methods

Reagents and solvents employed for the synthesis and purification of the target compounds (see Schemes 1–3) were available with purity >98% and purchased from Fluorochem, Sigma-Aldrich (St Louis, Missouri, United States) or Tokyo Chemical Industry Co., Ltd (TCI): 2-aminobenzoic acid (**1**), thiomorpholine (**2**), thiophen-2-ylmethanamine (**3**), thiophene-2-sulfonyl chloride (**7**), 2-(aminomethyl)aniline (**6**), 5-(dimethylamino)naphthalene-1-sulfonyl chloride (dansyl chloride) (**9**), methyl isothiocyanate (MeNCS), 2-(methylthio)aniline (**10**), 2-(1*H*-Benzotriazole-1-yl)-1,1,3,3-tetramethylaminium tetrafluoroborate (TBTU), *N*-Ethyldiisopropylamine (DIPEA), triethylamine (Et_3N), pyridine, methanol (MeOH), methyl *tert*-butyl ether (MTBE) and dichloromethane (DCM). Reagents and solvents required for the photophysical experiments: acetonitrile (CH_3CN) (Merck Millipore, Darmstadt, Germany, 99.5%, CAS 75-05-8); chloroform ($CHCl_3$) (Honeywell, Minneapolis, MN, USA, 99.0–99.4%, CAS 67-66-3); diemthylsulfoxyde (DMSO) (Honeywell, 99.5%, CAS 67-68-5); ethanol (EtOH) (Honeywell, 99.9%, CAS 64-17-5); tetrahydrofuran (THF) (PanReac, Barcelona, Spain, 99.0%, CAS 109-99-9); acetone (Honeywell, 99.5%, 67-64-1); ethylenediamine tetraacetic acid (EDTA) (Alfa Aesar, Ward Hill, MA, USA, CAS 194491-31-1); LUDOX® AS-30 colloidal silica (SiO_2, Sigma-Aldrich, 30 wt% suspension in water, CAS 7631-86-9); poly(methyl methacrylate) (PMMA) (Sigma-Aldrich, St, Louis, MO, USA, MW ~350,000, CAS 9011- 14-7); Zinc (II) trifluoromethanesulfonate (Sigma-Aldrich, St, Louis, MO, USA, CAS 54010-75-2); Silver (I) trifluoromethanesulfonate (Sigma-Aldrich, St, Louis, MO, USA, CAS 2923-28-6); Mercury (II) trifluoromethanesulfonate (Sigma-Aldrich, St, Louis, MO, USA, CAS 49540-00-3); Copper (II) trifluoromethanesulfonate (Sigma-Aldrich, St, Louis, MO, USA, CAS 34946-82-2); Acridine Yellow G (Sigma-Aldrich, St, Louis, MO, USA, CAS 135-49-9); hydrochloric acid 37% (Honeywell, CAS 7647-01-0); ammonia (Sigma-Aldrich, St, Louis, MO, USA, CAS 7664-41-7); H_2O (Milli-Q ultrapure).

The absorption spectra were recorded on a JASCO V-650 UV–Vis Spectrophotometer and the fluorescence emission spectra on a Horiba

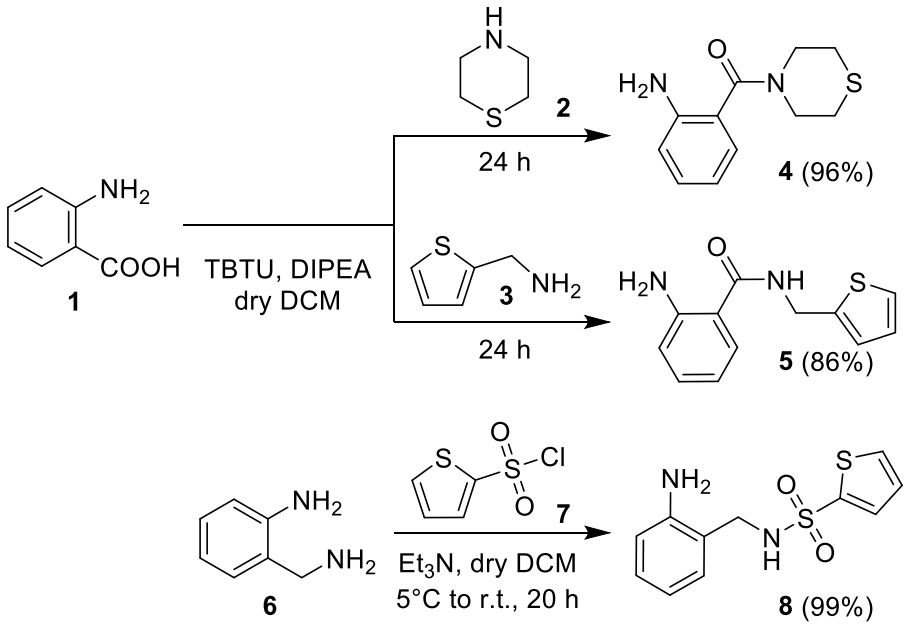

Scheme 1. Synthetic approach for the preparation of intermediates **4**, **5** and **8**.

Jobin-Yvon Scientific Fluoromax-4. Spectra of solid samples were collected with a Horiba-Jobin-Yvon Fluoromax-4® spectrofluorometer using an optic fibre connected to the equipment, by exciting the solid compounds at appropriated λ (nm). A correction for the absorbed light was performed when necessary. Lifetime studies were carried out on TemPro, Deltahub Nanoled of Horiba Jobin-Yvon, with a 390 nm Nanoled. All spectroscopic studies were performed using quartz cuvettes with a 10 mm optical path length. All analytical instruments were provided by PROTEOMASS-BIOSCOPE facility.

The chemical identities of all substances were confirmed through the utilization of various analytical techniques, including ^{1}H NMR, ^{13}C NMR, 2-D COSY, 2D-HSQC, and 2-D HMBC techniques. The ^{1}H NMR and ^{13}C NMR spectra were acquired on a Bruker Avance II^{+} 600 spectrometer using 5 mm tubes. The measurements were performed in $CDCl_3$ and DMSO-d_6 at a temperature of 293 K, with operating frequencies of 600.13 MHz and 150.92 MHz for ^{1}H and ^{13}C nuclei, respectively. The ^{1}H and ^{13}C nuclear magnetic resonance (NMR) spectra were standardized using the reference signal of tetramethylsilane (TMS) with a chemical shift value (δ) of 0.00. The precision of chemical changes is determined at a level of 0.01 ppm. The coupling constants (*J*) are displayed with a precision of 0.1 and denoted in units of hertz (Hz). The spin multiplicity observed in the ^{1}H nuclear magnetic resonance (NMR) spectroscopy was represented using the following abbreviations: s for singlet, d for doublet, t for triplet, q for quartet, dd for doublet of doublets, dt for doublet of triplets, td for triplet of doublets, and m for multiplet. MestreNova v. 14.1.1 (Mestrelab Research S.L.) was used for processing the spectra.

High-Resolution Mass Spectrometry analyses were carried out in the Laboratory for Biological Mass Spectrometry–Isabel Moura (PROTEOMASS Scientific Society Facility), using UHR ESI-Qq-TOF IMPACT HD (Bruker-Daltonics, Bremen, Germany). Compounds were dissolved in 50% (v/v) Acetonitrile containing 0.1% (v/v) aqueous formic acid to obtain a working solution of 0.1 μg/mL. Mass spectrometry analysis was carried out by the direct infusion of the compound solutions into the ESI source. MS data were acquired in positive polarity over the mass range of 80–1300 *m/z*. (Capillary voltage: 4500 V, End plate offset: −500 V, Charging voltage: 2000 V, Corona: 4000 nA, Nebulizer gas: 0.4 Bar, Dry Heater: 180 °C, Dry gas: 4.0 L/min).

2.2. Synthetic procedures

2.2.1. Synthetic procedures for intermediates *4, 5, 8, 12*

*2.2.1.1. Synthesis of (2-aminophenyl)(thiomorpholino)methanone (**4**).* To a solution of amino acid 1 (0.500 g, 3.65 mmol, 1.1 eq.) in 25 mL dry DCM were added at r.t. consequently DIPEA (1.21 mL, 7.29 mmol, 2.2 eq.), thiomorpholine 2 (0.33 mL, 3.31 mmol, 1.0 eq.) and TBTU (1.170 g, 3.65 mmol, 1.1 eq.). The formed clear solu-tion was stirred at r.t. for 24 h. Workup: reaction mixture was diluted with 40 mL DCM and consequently washed with aq. K_2CO_3 (x1) and water (x2). TLC – DCM: MTBE = 5:1, x2. Organic phase was dried over anhydr. Na_2SO_4 and evaporated *in vacuo* to dryness. The crude product was purified employing column chromatography: 40 g silica, mobile phase DCM: MTBE = 10:1, furnishing 0.700 g (96%) of compound **4** as pale yellow solid. ^{1}H NMR (600 MHz, $CDCl_3$) δ 7.17 (m, 1H), 7.05 (dd, *J* = 7.8, 1.6 Hz, 1H), 6.70–6.74 (m, 2H), 3.86 (br s, 4H), 2.66 (br s, 4H). ^{13}C NMR (151 MHz, $CDCl_3$) δ 170.3 (1C, C═O), 145.4, 130.7, 127.5, 119.7, 117.6, 116.8, 27.9.

*2.2.1.2. Synthesis of 2-amino-N-(thiophen-2-ylmethyl)benzamide (**5**).* To a solution of amino acid **1** (0.400 g, 2.92 mmol, 1.0 eq.) in 25 mL dry DCM were added at r.t. consequently DIPEA (1.21 mL, 7.29 mmol, 2.5 eq.), amine **3** (0.33 mL, 3.21 mmol, 1.1 eq.) and TBTU (1.030 g, 3.21 mmol, 1.1 eq.). The formed clear solution was stirred at r.t. for 24 h. Workup: reaction mixture was diluted with 40 mL DCM and washed consequently with aq. citric acid and water. TLC – DCM, x2. The organic phase was dried over anhydr. Na_2SO_4 and evaporated *in vacuo* to dryness. The crude product was purified by column chromatography: 40 g silica, mobile phase DCM, affording 0.580 g (86%) of compound **5** as a white solid. M.p. 111–112 °C. ^{1}H NMR (600 MHz, $CDCl_3$) δ 7.30 (dd, *J* = 7.9, 1.4 Hz, 1H), 7.24 (dd, *J* = 5.1, 1.1 Hz, 1H), 7.20 (ddd, *J* = 8.5, 7.2, 1.5 Hz, 1H), 7.02 (m, 1H), 6.97 (dd, *J* = 5.1, 3.5 Hz, 1H), 6.68 (dd, *J* = 8.1, 0.9 Hz), 6.62 (ddd, *J* = 8.1, 7.3, 1.1 Hz, 1H), 6.40 (br s, 1H, CO–N<u>H</u>), 5.54 (br s, 2H, N<u>H</u>$_2$), 4.76 (dd, *J* = 5.6, 0.6 Hz, 2H, C<u>H</u>$_2$). ^{13}C NMR (151 MHz, $CDCl_3$) δ 168.9 (1C, <u>C</u>═O), 148.9, 140.9, 132.5, 127.2, 126.9, 126.1, 125.3, 117.3, 116.6, 115.5, 38.5 (1C, <u>C</u>H$_2$).

*2.2.1.3. Synthesis of N-(2-aminobenzyl)thiophene-2-sulfonamide (**8**).* Diamine **6** (0.304 g, 2.49 mmol, 1.0 eq.) was dissolved in 25 mL dry

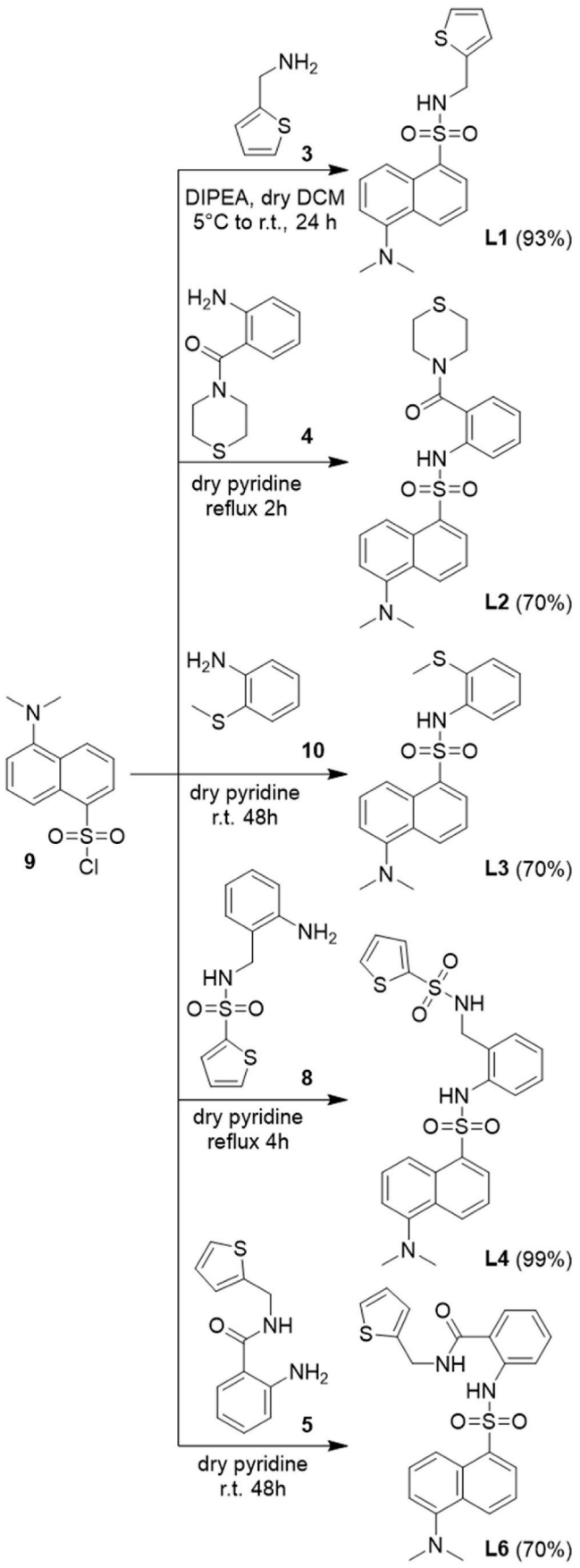

Scheme 2. Synthetic approach for the preparation of compounds **L1-L4** and **L6**.

DCM and Et_3N (0.42 mL, 2.99 mmol, 1.2 eq.) was added. The formed clear solution was cooled down to 5 °C (with water-ice) and sulfochloride **7** (0.500 g, 2.74 mmol, 1.1 eq.) was added portionwise. The resulting clear reaction mixture was stirred for 30 min at 5 °C followed by 20 h at r.t. Workup: the reaction mixture was diluted with 40 mL DCM and conse-quently washed with aq. citric acid and water. TLC – DCM, x2. The organic phase was dried over anhydr. Na_2SO_4 and evaporated *in vacuo* to dryness. The crude product was purified by column chromatography: 40 g silica, mobile phase DCM:MTBE = 20:1, to yield 0.670 g (99%) of compound **8** as white solid. M.p. 132–133 °C. ^{1}H NMR (600 MHz, $CDCl_3$) δ 7.62–7.66 (m, 2H), 7.10–7.14 (m, 2H), 6.93 (dd, J = 7.4, 0.9 Hz, 1H), 6.64–6.69 (m, 2H), 4.70 (t, J = 5.7 Hz, 1H, SO_2–N<u>H</u>), 4.10 (d, J = 6.2 Hz, 2H, C<u>H</u>$_2$), 4.03 (br s, 2H, N<u>H</u>$_2$). ^{13}C NMR (151 MHz, $CDCl_3$) δ 145.6, 139.9, 132.6, 132.3, 130.3, 129.9, 127.6, 119.2, 118.3, 116.3, 45.7 (1C, <u>C</u>H$_2$).

*2.2.1.4. Synthesis of N-(2-aminobenzyl)-5-(dimethylamino)naphthalene-1-sulfonamide (**12**).* To a solution of diamine **6** (0.400 g, 3.27 mmol, 1.0 eq.) in 25 mL dry DCM was added at r.t. Et_3N (0.59 ml, 4.26 mmol, 1.3 eq.). The formed clear solution was cooled to 5 °C (with water-ice) and dansyl chloride **9** (0.972 g, 3.60 mmol, 1.1 eq.) was added in portions. The formed clear yellow solution was stirred for 1 h at 5 °C, followed by20 h at r.t. Workup: reaction mixture was diluted with 40 mL DCM and washed with water. TLC – DCM:MTBE = 50:1, x2. The organic phase was dried over anhydr. Na_2SO_4 and evaporated *in vacuo* to dryness. The crude product was purified by column chromatography: 60 g silica; mobile phase DCM:MTBE = 50:1, affording 1.170 g (99%) of compound **12** as bright yellow solid. ^{1}H NMR (600 MHz, $CDCl_3$) δ 8.56 (m, 1H), 8.29 (dd, J = 7.3, 1.2 Hz, 1H), 8.26 (m, 1H), 7.52–7.57 (m, 2H), 7.19 (br d, J = 7.5 Hz, 1H), 7.04 (dt, J = 7.7, 1.4 Hz, 1H), 6.78 (dd, J = 7.9, 1.4 Hz, 1H), 6.55–6.58 (m, 2H), 4.87 (t, J = 6.1 Hz, 1H, SO_2N<u>H</u>), 3.93 (br s, 1H, N<u>H</u>$_2$), 3.91 (d, J = 6.1 Hz, 2H, C<u>H</u>$_2$), 2.90 (s, 6H, NMe_2). ^{13}C NMR (151 MHz, $CDCl_3$) δ 152.1, 145.6, 133.8, 130.8, 130.3, 130.2, 129.8, 129.6, 129.5, 128.6, 123.3, 119.5, 118.3, 118.1, 116.1, 115.3, 45.5 (1C, <u>C</u>H$_2$), 45.4 (2C, NMe_2).

*2.2.2. Synthetic procedures of compounds **L1** to **L6***

*2.2.2.1. Synthesis of 5-(dimethylamino)-N-(thiophen-2-ylmethyl)naphthalene-1-sulfonamide (**L1**).* To a solution of amine **3** (0.17 mL, 1.63 mmol, 1.1 eq.) in 20 mL dry DCM was added at r.t. DIPEA (0.31 mL, 1.78 mmol, 1.2 eq.). The formed clear solution was cooled down to 5 °C (with water-ice) and dansyl chloride **9** (0.400 g, 1.48 mmol, 1.0 eq.) was added in portions. The resulting clear yellow solution was stirred for 1 h at 5 °C, followed by 24 h at r.t. Workup: reaction mixture was diluted with 40 mL DCM and consequently washed with aq. citric acid and water. TLC – DCM, x2. Organic phase was dried over anhydr. Na_2SO_4 and evaporated *in vacuo* to dryness. The crude product was purified by column chromatography: 70 g silica; mobile phase DCM. After column purification, the product was washed with 3 mL of hot petroleum ether, cooled down to r.t., decanted and dried *in vacuo* to give 0.480 g (93%) of pure **L1** as pale yellow powder. M.p. 113–114 °C. ^{1}H NMR (600 MHz, $CDCl_3$) δ 8.54 (dt, J = 8.5, 1.1 Hz, 1H, H-10), 8.26 (tt, J = 7.1, 1.1 Hz, 2H, H-3 and H-8 overlapped), 7.56 (dd, J = 8.6, 7.5 Hz, 1H, H-2), 7.52 (dd, J = 8.5, 7.2 Hz, 1H, H-9), 7.19 (dd, J = 7.6, 0.9 Hz, 1H, H-1), 7.09 (dd, J = 5.1, 1.2 Hz, 1H, H-21), 6.77 (dd, J = 5.1, 3.5 Hz, 1H, H-22), 6.72 (dt, J = 3.5, 1.0 Hz, 1H, H-23), 4.94 (t, J = 6.0 Hz, 1H, N<u>H</u>), 4.28 (dd, J = 6.2, 0.9 Hz, 2H, H-18), 2.90 (s, 6H, NMe_2). ^{13}C NMR (151 MHz, $CDCl_3$) δ 152.0 (1C, C-6), 138.7 (1C, C-19), 134.4 (1C, C-7), 130.7 (1C, C-10), 129.9 (2C, C-4 and C-5 overlapped), 129.6 (1C, C-2), 128.5 (1C, C-8), 126.7 (1C, C-22), 126.5 (1C, C-23), 125.7 (1C, C-21), 123.2 (1C, C-9), 118.6 (1C, C-3), 115.2 (1C, C-1), 45.4 (2C, NMe_2), 42.2 (1C, C-18). (Figures S1-1 to S1-18). ESI-MS: [M+H]+ for $C_{17}H_{19}N_2O_2S_2$ = 347.0882 (−0.1 ppm). Calculated [M+H]+ for $C_{17}H_{19}N_2O_2S_2$ = 347.0882.

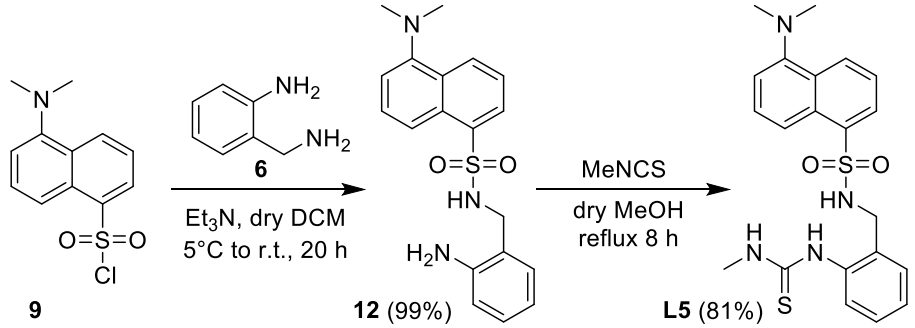

Scheme 3. Synthesis of intermediate **12** and target compound **L5**.

*2.2.2.2. Synthesis of 5-(dimethylamino)-N-(2-(thiomorpholine-4-carbonyl)phenyl)naphthalene-1-sulfonamide (**L2**).* To 10 mL dry pyridine was added intermediate **4** (0.700 g, 3.15 mmol, 1.0 eq.) and dansyl chloride **9** (1.020 g, 3.78 mmol, 1.2 eq.). The reaction mixture was gently refluxed at 115 °C for 2 h (until exhaustion of **4**). TLC – DCM: MTBE = 50:1, x2. Workup: reaction mixture was diluted with 70 mL DCM and consequently washed with aq. citric acid (x2) and water (x2). The organic phase was dried over anhydr. Na_2SO_4 and evaporated *in vacuo* to dryness. The crude product was purified by column chromatography: 60 g silica; mobile phase DCM:MTBE = 50:1. After purification by column the product was washed with 3 mL hot petroleum ether, cooled down to r.t., decanted and dried *in vacuo* to give 1.000 g (70%) of compound **L2** as light yellow powder. M.p. 176–177 °C. ^{1}H NMR (600 MHz, $CDCl_3$) δ 8.68 (s, 1H, NH), 8.50 (dt, *J* = 8.6, 1.1 Hz, 1H, H-10), 8.33 (dt, *J* = 8.6, 1.0 Hz, 1H, H-3), 8.13 (dd, *J* = 7.3, 1.3 Hz, 1H, H-8), 7.77 (dd, *J* = 8.4, 1.1 Hz, 1H, H-23), 7.63 (dd, *J* = 8.7, 7.5 Hz, 1H, H-2), 7.41 (dd, *J* = 8.5, 7.3 Hz, 1H, H-9), 7.34 (ddd, *J* = 8.6, 7.4, 1.6 Hz, 1H, H-22), 7.28–7.22 (m, 1H, H-1), 7.03 (td, *J* = 7.5, 1.2 Hz, 1H, H-21), 6.93 (dd, *J* = 7.7, 1.6 Hz, 1H, H-20), 3.50 (s, 2H, aliphatic CH_2), 2.88 (s, 6H, NMe_2), 2.69 (s, 2H, aliphatic CH_2), 2.46 (br s, 2H, aliphatic CH_2), 2.02 (br s, 2H, aliphatic CH_2). ^{13}C NMR (151 MHz, $CDCl_3$) δ 168.6 (1C, C=O), 152.1 (1C, C-6), 136.1 (1C, C-18), 134.5 (1C, C-7), 131.0 (1C, C-22), 130.7 (1C, C-10), 130.1 (1C, C-2), 129.9 (1C, C-4), 129.2 (1C, C-5), 128.6 (1C, C-8), 127.2 (1C, C-20), 125.8 (1C, C-19), 124.3 (1C, C-23), 124.1 (1C, C-21), 123.2 (1C, C-9), 118.9 (1C, C-3), 115.7 (1C, C-1), 45.2 (2C, br s, C-27 and C-31), 44.7 (2C, NMe_2), 27.3 (2C, C-28 and C-30). (Figures S2-1 to S2-13). ESI-MS: [M+H]+ for $C_{23}H_{26}N_3O_3S_2$ = 456.1407 (−0.7 ppm). Calculated [M+H]+ for $C_{23}H_{26}N_3O_3S_2$ = 456.1410.

*2.2.2.3. Synthesis of 5-(dimethylamino)-N-(2-(methylthio)phenyl)naphthalene-1-sulfonamide (**L3**).* To 4 mL dry pyridine were added amine **10** (0.338 g, 2.43 mmol, 1.0 eq.) and dansyl chloride **9** (0.786 g, 2.91 mmol, 1.2 eq.). The reaction mixture was stirred at r.t for 48 h (until exhaustion of **10**). TLC – DCM:PE = 1:1, x2. Workup: the reaction mixture was diluted with 50 mL DCM and consequently washed with 2 N HCl and water. The organic phase was dried over anhydr. Na_2SO_4 and evaporated *in vacuo* to dryness. The crude product was purified by column chromatography: 70 g silica; mobile phase DCM. After column product was washed with 3 mL hot petroleum ether, cooled down to room temperature, decanted and dried *in vacuo* affording 0.640 g (70%) of compound **L3** as yellow powder. M.p. 101–102 °C. ^{1}H NMR (600 MHz, $CDCl_3$) δ 8.50 (dt, *J* = 8.5, 1.1 Hz, 1H, H-10), 8.39 (dd, *J* = 8.7, 1.0 Hz, 1H, H-3), 8.29 (dd, *J* = 7.3, 1.3 Hz, 1H, H-8), 8.15 (br s, 1H, NH), 7.57 (dd, *J* = 8.7, 7.5 Hz, 1H, H-2), 7.51–7.44 (m, 2H, H-9 and H-21 overlapped), 7.32 (dd, *J* = 7.7, 1.6 Hz, 1H, H-23), 7.18–7.13 (m, 2H, H-1 and H-20 overlapped), 6.93 (td, *J* = 7.6, 1.3 Hz, 1H, H-22), 2.84 (s, 6H, NMe_2), 2.03 (s, 3H, S–Me). ^{13}C NMR (151 MHz, $CDCl_3$) δ 152.0 (1C, C-6), 137.9 (1C, C-18), 134.2 (1C, C-22), 134.1 (1C, C-7), 131.0 (1C, C-10), 130.4 (1C, C-8), 129.8 (1C, C-4), 129.5 (1C, C-5), 129.2 (1C, C-20), 128.6 (1C, C-2), 125.8 (1C, C-19), 124.4 (1C, C-23), 123.0 (1C, C-9), 118.7 (1C, C-3), 118.5 (1C, C-21), 115.3 (1C, C-1), 45.4 (2C, NMe_2), 19.6 (1C, S–Me). (Figures S3-1 to S3-12). ESI-MS: [M+H]+ for $C_{19}H_{21}N_2O_2S_2$ = 373.1050 (3 ppm). Calculated [M+H]+ for $C_{19}H_{21}N_2O_2S_2$ = 373.1039.

*2.2.2.4. Synthesis of N-(2-((5-(dimethylamino)naphthalene)-1-sulfonamido)benzyl)thiophene-2-sulfonamide (**L4**).* To 10 mL dry pyridine were added intermediate **8** (0.300 g, 1.12 mmol, 1.0 eq.) and dansyl chloride **9** (0.362 g, 1.34 mmol, 1.2 eq.). The reaction mixture was gently refluxed at 115 °C for 4 h (until exhaustion of **8**). TLC – DCM:PE = 1:1, x2. Workup: the reaction mixture was diluted with 70 mL DCM and consequently washed with aq. citric acid (x3) and water (x2). Organic phase was dried over anhydrous Na_2SO_4 and evaporated *in vacuo* to dryness. The crude product was purified by column chromatography: 70 g silica; mobile phase DCM:MTBE = 100:1. After column chromatography, the product was washed with 3 mL hot petroleum ether, cooled down to r.t., decanted and dried *in vacuo* to give 0.560 g (99%) of compound **L4** as yellow powder. M.p. 83–84 °C. ^{1}H NMR (600 MHz, $CDCl_3$) δ 8.52 (dt, *J* = 8.5, 1.2 Hz, 1H, H-10), 8.31 (dd, *J* = 8.7, 1.0 Hz, 1H, H-3), 8.09 (dd, *J* = 7.3, 1.3 Hz, 1H, H-8), 7.63 (s, 1H, SO_2–NH-Ar), 7.62 (q, *J* = 1.4 Hz, 1H, H-20), 7.58 (dd, *J* = 8.7, 7.5 Hz, 1H, H-2), 7.43 (dd, *J* = 8.5, 7.3 Hz, 1H, H-9), 7.21 (br s, 1H, CH-thiophene), 7.19 (dd, *J* = 7.7, 0.9 Hz, 1H, H-1), 7.17 (dd, *J* = 7.5, 1.7 Hz, 1H, CH-thiophene), 7.11 (dd, *J* = 4.9, 3.9 Hz, 1H, H-21), 7.04 (td, *J* = 7.5, 1.4 Hz, 1H, H-22), 6.99 (td, *J* = 7.7, 1.7 Hz, 1H, H-23), 6.72 (dd, *J* = 8.0, 1.4 Hz, 1H, H-32), 5.26 (t, *J* = 6.6 Hz, 1H, SO_2–NH–CH_2), 4.07 (d, *J* = 6.6 Hz, 2H, H-24), 2.89 (s, 6H, NMe_2). ^{13}C NMR (151 MHz, $CDCl_3$) δ 152.1 (1C, C-6), 140.1 (1C, C-19), 134.8 (1C, C-18), 133.9 (1C, C-7), 132.6 (1C, CH-thiophene), 132.3 (1C, C-20), 131.0 (1C, CH-thiophene), 131.0 (1C, C-10), 130.7 (1C, C-27), 130.6 (1C, C-8), 129.7 (1C, C-4), 129.5 (1C, C-5), 129.2 (1C, C-23), 128.9 (1C, C-2), 127.6 (1C, C-21), 126.7 (1C, C-22), 124.7 (1C, C-32), 123.1 (1C, C-9), 118.5 (1C, C-3), 115.3 (1C, C-1), 45.4 (2C, NMe_2), 44.3 (1C, C-24). (Figures S4-1 to S4-13). ESI-MS: [M+H]+ for $C_{23}H_{24}N_3O_4S_3$ = 502.0938 (2.9 ppm). Calculated [M+H]+ for $C_{23}H_{24}N_3O_4S_3$ = 502.0923.

*2.2.2.5. Synthesis of 5-(dimethylamino)-N-(2-(3-methylthioureido)benzyl) naphthalene-1-sulfonamide (**L5**).* A solution of **12** (0.410 g, 1.15 mmol, 1.0 eq.) and methyl isothiocyanate (0.168 g, 2.30 mmol, 2.0 eq.) in 10 mL dry MeOH was gently refluxed for 8 h (until exhaustion of **12**). TLC – DCM:MTBE = 20:1, x2. Workup: the solvent was evaporated to dryness and the rest was purified using column chromatography: 60 g silica; mobile phase DCM:MTBE = 20:1. After the column purification, the product was washed with 3 mL hot petroleum ether, cooled down to room temperature, decanted and dried *in vacuo* furnishing 0.400 g (81%) of compound **L5** as yellow powder. M.p. 99–100 °C. ^{1}H NMR (600 MHz, DMSO-d_6) δ 8.72 (br s, 1H, SO_2–NH), 8.47 (dt, *J* = 8.5, 1.0 Hz, 1H, H-10), 8.36 (dt, *J* = 8.7, 0.9 Hz, 1H, H-3), 8.12 (dd, *J* = 7.3, 1.3 Hz, 1H, H-8), 7.95 (br s, 1H, Ar-NH-CS), 7.58 (m, 2H, H2 and H-9 overlapped), 7.27 (m, 3H, H-1, H-24 and CH_3–NH overlapped), 7.19 (td, *J* = 7.6, 1.6 Hz, 1H, H-22), 7.12 (dd, *J* = 7.9, 1.4 Hz, 1H, H-21), 7.08 (td,

J = 7.5, 1.4 Hz, 1H, H-23), 4.05 (br s, 2H, H-18), 2.86 (s, 6H, NMe_2), 2.86 (d, J = 2.4 Hz, 3H, CH_3–NH). ^{13}C NMR (151 MHz, DMSO-d_6) δ 182.4 (1C, C=S), 151.1 (1C, C-6), 135.9 (1C, C-20), 134.2 (1C, C-7), 123.0 (1C, C-10), 1 29.0 (1C, C-4), 128.9 (1C, C-5), 128.0 (1C, C-8), 127.8 (1C, C-24), 127.5 (1C, C-19), 127.3 (1C, C-21), 127.1 (1C, C-22), 125.9 (1C, C-23), 123.0 (1C, C-9), 118.8 (1C, C-3), 114.8 (1C, C-1), 44.6 (2C, NMe_2), 42.0 (1C, C-18), 30.7 (1C, C-29). (Figures S5-1 to S5-13). ESI-MS: [M+H]+ for $C_{21}H_{25}N_4O_2S_2$ = 429.1425 (2.7 ppm). Calculated [M+H]+ for $C_{21}H_{25}N_4O_2S_2$ = 429.1413.

*2.2.2.6. Synthesis of 2-((5-(dimethylamino)naphthalene)-1-sulfonamido)-N-(thiophen-2-ylmethyl)benzamide (**L6**).* To 5 mL dry pyridine was added intermediate **5** (0.250 g, 1.08 mmol, 1.0 eq.) and dansyl chloride **9** (0.348 g, 1.29 mmol, 1.2 eq.). The reaction mixture was stirred at r.t for 48 h (until exhaustion of **5**). TLC – DCM, x2. Workup: the reaction mixture was diluted with 70 mL DCM and consequently washed with 2 N HCl (x1) and water (x2). The organic phase was dried over anhydr. Na_2SO_4 and evaporated *in vacuo* to dryness. The crude product was purified by column chromatography: 70 g silica; phase DCM:MTBE = 100:1. After column product was washed with 3 ml hot PE, cooled, decanted, and dried *in vacuo* yielding 0.350 g (70%) of compound **L6** as yellow powder. M.p. 210–211 °C. ^{1}H NMR (600 MHz, $CDCl_3$) δ 11.18 (s, 1H, SO_2–NH), 8.48 (dt, J = 8.5, 1.2 Hz, 1H, H-16), 8.38 (d, J = 8.7 Hz, 1H, H-22), 8.26 (dd, J = 7.3, 1.3 Hz, 1H, H-14), 7.60 (dd, J = 8.4, 1.1 Hz, 1H, H-7), 7.55 (dd, J = 8.7, 7.6 Hz, 1H, H-21), 7.44 (dd, J = 8.5, 7.3 Hz, 1H, H-15), 7.29 (ddd, J = 8.6, 7.4, 1.5 Hz, 1H, H-6), 7.26–7.21 (m, 2H, H-4 and H-31 overlapped), 7.14 (d, J = 7.3 Hz, 1H, H-20), 6.96 (d, J = 3.4 Hz, 2H, H-30 and H-32 overlapped), 6.90 (td, J = 7.6, 1.1 Hz, 1H, H-5), 6.20 (br t, J = 5.4 Hz, 1H, CO–NH), 4.55 (d, J = 5.5 Hz, 2H, H-27), 2.84 (s, 6H, NMe_2). ^{13}C NMR (151 MHz, $CDCl_3$) δ 167.9 (1C, C=O), 151.7 (1C, C-19), 139.6 (1C, C-28), 138.9 (1C, C-8), 134.6 (1C, C-11), 132.7 (1C, C-6), 130.7 (1C, C-16), 130.1 (1C, C-14), 129.8 (1C, C-17), 129.5 (1C, C-18), 128.4 (1C, C-21), 127.0 (1C, C-31), 126.6 (1C, C-4), 126.6 (1C, C-32), 125.6 (1C, C-30), 123.0 (1C, C-15), 122.8 (1C, C-5), 120.4 (1C, C-2), 119.9 (1C, C-7), 119.2 (1C, C-22), 115.3 (1C, C-20), 45.4 (2C, NMe_2), 38.6 (1C, C-27). (Figures S6-1 to S6-16). ESI-MS: [M+H]+ for $C_{24}H_{24}N_3O_3S_2$ = 466.1253 (−0.1 ppm). Calculated [M+H]+ for $C_{24}H_{24}N_3O_3S_2$ = 466.1254.

2.3. Spectrophotometric and spectrofluorimetric measurements

The spectroscopic characterizations and titrations were performed using stock solutions of the compounds (ca. 10^{-3} M), prepared by dissolving the appropriate amounts of each compound **L1**-**L6** in acetonitrile, chloroform, dimethyl sulfoxide, tetrahydrofuran, and ethanol. The studied solutions were prepared by appropriate dilution of the stock solutions up to 10^{-5}–10^{-6}. Titrations of compounds **L1**-**L6** were carried out in acetonitrile by the addition of microliter amounts of standard metal solutions of Zn^{2+}, Ag^{+}, Hg^{2+} and Cu^{2+} in acetonitrile and HCl and NH_3 in H_2O. The complexation constants for the interaction of ligands **L1** to **L6** in the presence of Hg^{2+} and Cu^{2+} metal ions were calculated using the *HypSpec* software [22]. Luminescence quantum yield of compounds **L1**-**L6** was measured using a solution of Acridine Yellow [φ = 0.37] [23,24] in ethanol as standard. All measurements were performed at 298 K.

2.4. Dye doped PMMA polymeric films

The doped polymer films were obtained at room temperature by dissolving 100 mg of PMMA in 5 mL of chloroform, followed by the addition of 1 mg of each compound **L1-L6,** previously dissolved in 1 mL of chloroform. The polymer films were obtained after slow evaporation at room temperature (24 h).

2.5. Acidity assays

The reactivity and resistance of the dye-doped polymers to HCl and vapours were tested by dipping the polymer in a 2–12 M gradient and into vapours of concentrated HCl. The reproducibility of the dye-doped polymers was proved by continuous immersion of the polymers in HCl and ammonia for ten cycles.

The changes in the polymers were spectroscopically analyzed.

3. Results and discussion

3.1. Synthesis

A series of six dansyl derivatives **L1**-**L6** were prepared (Schemes 1–3), and their photophysical properties were examined in current investigation. According to databases, five of them are new. Only compound **L1** was obtained earlier, in a publication concerning the development of new method for the synthesis of sulfonamides from benzylic alcohols [25]. However, the photophysical properties of this compound were not subjected to further studies.

The synthesis of three intermediates **4**, **5** and **8** from commercially available reagents was performed (Scheme 1). These intermediate products were obtained quantitatively and used in the next steps for the synthesis of the target compounds. Compound **4** was prepared under basic conditions, through a reaction between anthranilic acid (**1**) and thiomorpholine in the presence of coupling reagent TBTU. Amide **5** was prepared in a similar manner from **1** and amine **3**. Amide **8** was obtained also by selective acylation of diamine **6** with sulfochloride **7** (Scheme 3). The coupling reactions occur selectively towards the aliphatic amino group, which is not unusual [26]. Thus, due to stronger nucleophilicity of aliphatic amino groups in reagents **2**, **3** and **6** there is no need for protection of the aromatic groups of **1** and **6**. Amides **4**, **5** and **8** were observed as single step reaction products.

Intriguingly, the preparation and structural characterization of **4** [27] and **5** [26,28–31] was already described in earlier studies. However, different syn-thetic methods were employed – aminolysis of isatoic anhydride with amines **2** and **3**, respectively. The preparation of intermediate **12** starting from commercially available dansyl chloride (**9**) and diamine **6** (Scheme 3) was performed by implementation of an existing protocol [32].

The synthesis of amide **L1** (Scheme 2) was accomplished by one step acylation of amine **3** with **9** in the presence of DIPEA. Other target compounds (**L2-L4** and **L6**) were prepared by acylation of the above mentioned intermediates (**4**, **5** and **8**) or the commercially available amine **10** with dansyl chloride (**9**) in dry pyridine. The reaction outcome was monitored using TLC until starting reagents exhausted. Compound **L5** was prepared by addition of methyl isothiocyanate to intermediate **12** in refluxing methanol (Scheme 3), as Ambati et al. described for similar compounds [33]. All target compounds **L1-L6** were obtained quantitatevely. Due to steric hindrance (as in the case of compound **L2**) or possible tautomerism (in the case of **L5**), NMR spectra of both compounds at room temperature were not informative enough. Thus, they were performed at 353 K aiming to obtain narrow signals.

3.2. Photophysical characterization

The absorption and emission spectra of all six dansyl derivatives **L1**-**L6** were studied in five different solvents, namely, DMSO, CH_3CN, EtOH, THF and $CHCl_3$ at 298 K (Figs. S8–S13). Additionally, the emission solid state spectra were also obtained for these derivatives. The main results are summarized in Fig. 1 and Table 1.

Selecting acetonitrile as a representative solvent, all compounds exhibited an absorption band at 341 nm, 345 nm, 320 nm, 345 nm, 337 nm, 333 nm, from **L1** to **L6**, characteristic of the π - π* transition of the dansyl chromophores (see Table 2). These compounds appear colorless to the naked eye. However, upon emission, they display a pronounced

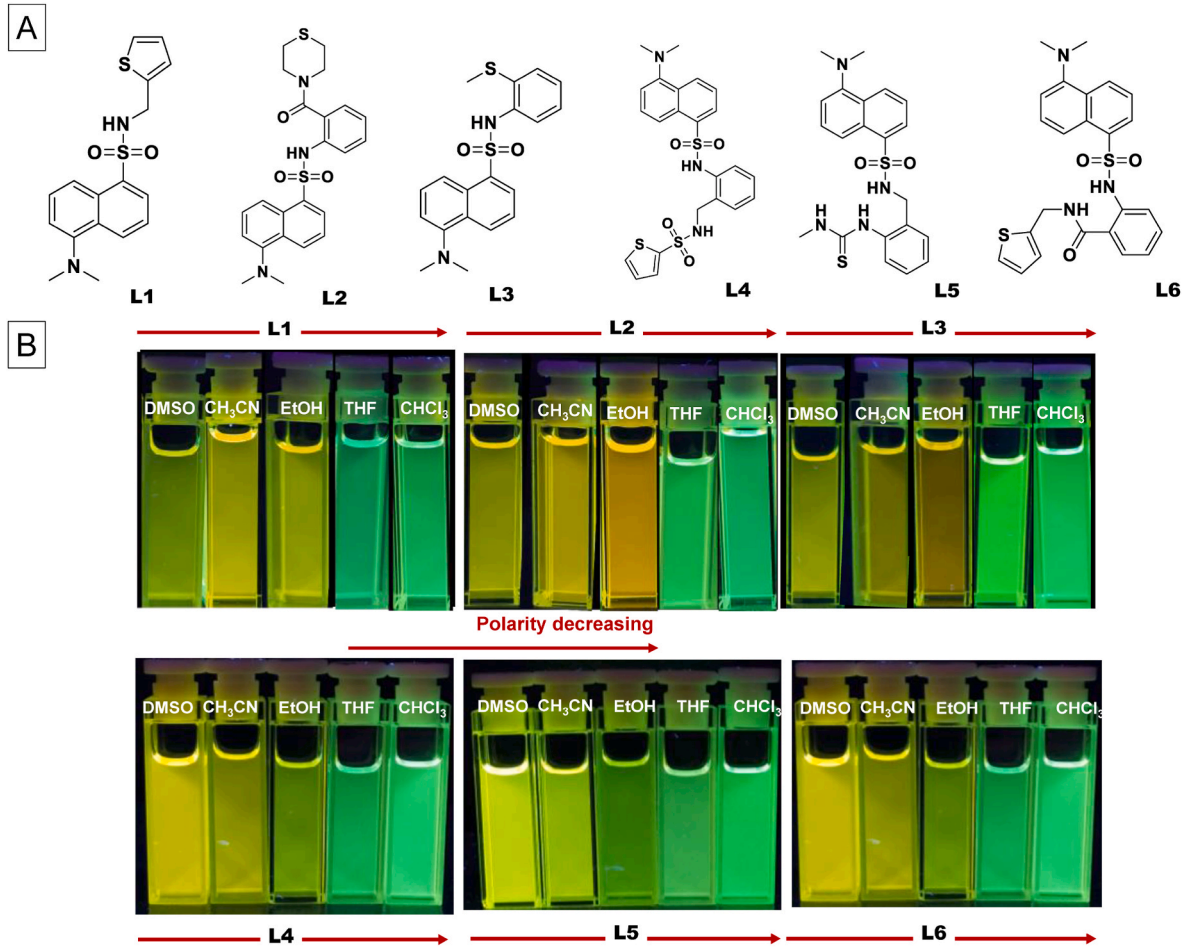

Fig. 1. (A) Chemical structures of dansyl-derivatives **L1**-**L6**. (B) Images of **L1**-**L6** under a UV light lamp. Polarity decreasing from DMSO to $CHCl_3$. [L] = 20 μM, T = 298 K.

Table 1
Spectroscopic polarity parameters, physical properties of the different solvents. ε_r: relative permittivity; η: refractive index; α: the solvent's HBD acidity; β: the solvent's HBA basicity; π*: the solvent's dipolarity/polarizability.

Solvent	ε_r	α	β	π*	η
DMSO	47.24	0	0.76	1.00	1.47
CH_3CN	35.94	0.19	0.40	0.66	1.34
EtOH	24.30	0.86	0.75	0.54	1.36
THF	7.58	0	0.55	0.58	1.40
$CHCl_3$	4.89	0.20	0.10	0.69	1.44

yellow emission, with maximum bands at 519, 528, 535, 530, 520 and 528 nm, from **L1** to **L6**, respectively. Specifically, **L2**, **L3**, **L4** and **L6**, which have a benzene unit directly attached to the dansyl unit, do not exhibit significant changes were observed in the excited state, with maximum emission value ca. 528–530 nm. The same was not verified in the ground state where the increase of donor atoms and side chain length promotes a red shift in the maximum bands, ranging from 320 nm to 345 nm. In contrast, **L1** and **L5**, which have a spacer between the dansyl chromophores, showed a blue shift of ca. 10 nm in the emission bands (*ca.* 519–520 nm), but no significant changes in the absorption.

For solid-state emissions, **L4** and **L5** exhibit emission bands at a longer wavelength (*ca.* 500–505 nm) than the other compounds (*ca.* 478–486 nm), probably due to their higher number of donor atoms. **L1** and **L5** demonstrate the highest fluorescence quantum yield (φ = *ca.* 35–36%), suggesting that the introduction of a spacer might stabilize these molecules in their excited state.

Although the solvatochromism effect is a well documented observation for dansyl molecules, our interest was to understand the influence that the different substituents may provide over this behaviour. As solvent polarity decreased, a change in emission color from yellow to green was noted. This change was due to a red shift in the maximum emission bands, varying from 496 to 522 nm for **L1**, 499 nm–540 nm for **L2**, 503–536 nm for **L3**, 504–533 nm for **L4**, 500 nm–524 nm to **L4** and 497 nm–537 nm for **L6**, respectively. In the absorption no significant correlation is identified.

Based on previous studies from our group it is evident that solvents with greater polarity significantly influence the stability of molecules. From the observed shifts, all compounds display a pronounced positive solvatochromic effect, suggesting enhanced stabilization of their excited state in highly polar solvents. This behavior provides an opportunity to stimulate the properties of the compound's microenvironment, offering potential applications in determining the local polarity in membranes, proteins, DNA [34]. Furthermore, this phenomenon can be valuable in understanding the characteris-tics of ionic liquids or mixed solvents and hold importance in the textile industry [35].

To quantitatively understand the interactions between solute and solvent, a multiparametric fit using the Kamlet-Taft equation was carried out (Equation (1)). This equation enabled the determination of certain solute-dependent parameters which relate to solvent properties such as hydrogen bond donating (HBD) acidity (α), hydrogen bond accepting (HBA) basicity (β), and the solvent's dipolarity/polarizability (π*).

$$\upsilon = \upsilon_0 + a\alpha + b\beta + p\pi^* \qquad \text{(Equation 1)}$$

Table 2
Photophysical characterization data of dansyl derivatives **L1-L6** in the different solvents.

Cpd.	Solv.	λ_{abs} [nm]	λ_{em} [nm]	ε [10^3 cm^{-1} M^{-1}]	Stokes shift [cm^{-1}]	$\lambda_{em.solid}$ [nm]	Φ (%)	Brightness (ε X φ) [cm^{-1} M^{-1}]	t[ns]
L1	DMSO	337	522	5.78	10500	484	22	1300	17
	CH_3CN	341	519	5.50	10100		35	1900	10
	EtOH	335	516	4.90	10500		31	1500	13
	THF	334	498	4.97	9860		21	1000	12
	$CHCl_3$	345	496	4.72	8820		35	1700	14
L2	DMSO	353	540	5.95	9810	478	11	670	13
	CH_3CN	345	528	5.52	10000		29	1600	12
	EtOH	346	520	4.98	9670		38	1900	13
	THF	334	504	5.20	10100		39	2000	13
	$CHCl_3$	345	499	5.20	8940		37	2000	15
L3	DMSO	340	536	5.40	10800	486	10	550	13
	CH_3CN	320	535	5.45	12600		28	1500	11
	EtOH	340	531	5.05	10600		32	1600	11
	THF	339	511	4.92	9930		32	1600	13
	$CHCl_3$	346	503	4.06	9020		32	1300	15
L4	DMSO	343	533	4.25	10400	505	21	910	15
	CH_3CN	345	530	4.47	10100		27	1200	10
	EtOH	345	522	3.78	9830		17	650	13
	THF	343	502	4.65	9230		27	1300	13
	$CHCl_3$	345	504	4.48	9140		29	1300	15
L5	DMSO	339	524	4.64	10400	500	30	1400	17
	CH_3CN	337	520	5.67	10400		36	2000	11
	EtOH	338	515	3.97	10200		22	900	13
	THF	337	497	4.94	9550		26	1300	13
	$CHCl_3$	343	500	3.59	9160		34	1200	15
L6	DMSO	347	537	4.28	10200	486	17	740	14
	CH_3CN	333	528	4.82	11100		28	1400	11
	EtOH	329	525	7.16	11300		17	1200	13
	THF	341	501	4.37	9360		29	1300	13
	$CHCl_3$	341	497	4.78	9200		34	1600	14

where υ_0 is the value of emission in a reference solvent. (see Table 1) [35].

Table 3 shows the fitted parameters (υ_0, a, b and p), the slope and correlation coefficients based on the fitting linear plots of $\upsilon_{exp.}$ versus υ_{calc}.

Analysis of the results in Table 3, clearly evidences that the solvatochromic effect is essential due to higher sensitivity to H-bond acceptor (or electron donor) strength of the solvents, as can be observed in the b values, with one-order of magnitude higher than a, respectively. However, the values indicate an even stronger influence of the solvent's dipolarity/polarizability with p values with one and two orders of magnitude higher than a. Thus, electronic interactions (polarity and polarizability) and hydrogen bond accepting behavior of the solvent play a dominant role compared to its hydrogen bond donating character.

3.3. Metal sensing ability

The sensorial ability of dansyl derivatives **L1**-**L6** towards Zn^{2+}, Cu^{2+}, Hg^{2+}, Ag^{+} metal ions in acetonitrile, was evaluated by titrating the free ligand with small amounts of the metal ions. The absorption and emission spectra were collected at 298 K until reaching a plateau. From the studied metal ions, all dansyl derivatives showed to only sense Cu^{2+} and Hg^{2+} metal ions, as already verified in our previous studies [7,8]. The spectral behavior was quite similar between ligands, thus as a representative example the dansyl derivatives **L1** and **L5** were selected. **L5** despite less intensive also revealed an interesting sensibility to Ag^{+} metal ions. Titrations with the other ligands are presented in Supplementary Material (Figs. S14–S18). Fig. 2 shows the absorption and emission spectral changes of **L1** upon coordination with Cu^{2+} metal ions, in acetonitrile. When increasing of Cu^{2+} and Hg^{2+} concentration similar spectral behavior in the absorption is noticed, resulting on a decrease in the absorption at 341 nm from both, and an increase in the absorbance at 298 nm and 287 nm for Cu^{2+} and Hg^{2+}, respectively. The emission spectra a fast decrease in the emission intensity at 519 nm is detected in both cases. Cu^{2+} metal ions, as a paramagnetic transition metal ion has unfilled *d* orbital shells. This characteristic makes it particularly susceptible to the chelation enhancement of quenching (CHEQ effect). The causing mechanisms driving this effect can be electron transfer or energy transfer.

Conversely, Hg^{2+} presents a unique case. While it is a diamagnetic metal with a filled d^{10} configuration, its quenching behaviour is not analogous to typical diamagnetic ions. The primary reason could be Spin-Orbit coupling due to its large atomic number, causing more predominant non-radiative deactivation pathways, which can also be induced by the formation of heavy atom complexes [36–38].

Fig. 3 presents the absorption and emission titrations of **L5** in response to the addition of Cu^{2+}, Hg^{2+} and Ag^{+} metal ions. The spectral patterns observed are consistent with those seen for the other ligands, with a notable exception for Ag^{+} where a quenching in the emission intensity is also detected. In this case, no spectral changes were observed in the ground state. The observed emission quenching can be attributed probably to the photoinduced electron transfer effect induced by Ag^{+}, which is consistent with the **L5** structure where the number of nitrogen atoms is higher and not all protected by complexation.

In order to provide more insights into the interactions between the dansyl derivatives **L1**-**L6** with the tested metal ions and quantify the

Table 3
υ_0, a, b and p-values, in cm^{-1}, slope and correlation coefficients obtained from Kamlet–Taft multiparametric fitting of the emission data.

	υ_0	a	b	p	Slope	R^2
L1	33032	−533	−4770	−17808	1.00	1
L2	35386	−350	−5804	−21300	1.00	1
L3	35354	−432	−6116	−21414	1.00	1
L4	35581	−638	−5444	−21838	1.00	1
L5	32841	−629	−4363	−17796	1.00	1
L6	36665	−672	−6248	−22877	1.00	1

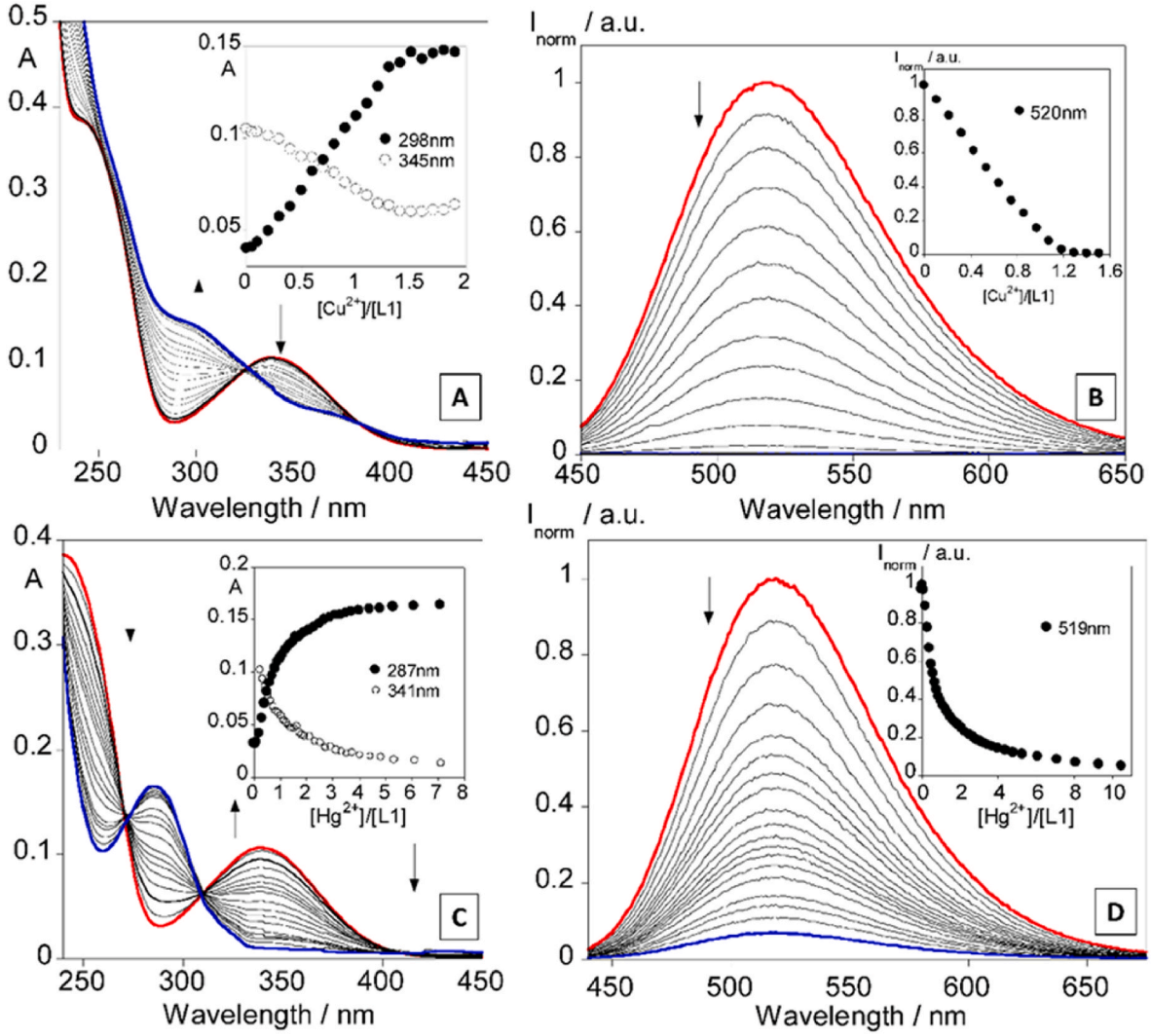

Fig. 2. Spectrophotometric and spectrofluorometric titrations of dansyl derivative **L1** with increased additions of Cu^{2+} (A, B), and Hg^{2+} (C, D) in CH_3CN. The inset represents the absorption (A, C) and emission (B,D) as a function of $[Cu^{2+}]/[\mathbf{L1}]$ and $[Hg^{2+}]/[\mathbf{L1}]$, respectively. $[\mathbf{L1}] = 20\ \mu M$, $\lambda_{exc\mathbf{L1}} = 341$ nm, T = 298 K).

strength of these interactions, their stability constants were determined using the HypSpec program [22]. The summarized results are presented in Table 4.

The stability constants indicate the formation of mononuclear species for Cu^{2+} and Hg^{2+} in the case of **L1-L6** and also for Ag^{+} in the case of compound **L5**. Notably, **L3** exhibits the highest stability constant among the derivatives with a value of $LogK_{ass.} = 11.40 \pm 0.02$ for its interaction with Cu^{2+}. We can observe that compounds **L1**, **L2**, and **L3** exhibit higher stability constants towards Cu^{2+} and Hg^{2+} than compounds **L4**, **L5** and **L6**. This variety of results may be attributed to the type of available coordinating groups, as well the position of their corresponding heteroatoms. The differences observed for these first three compounds can be highlighted by the high steric hindrance of the sulfur atom of the thiophene group decreasing to the largest extent the stability association constant among these. A better association constant is provided by **L2** with a possible coordination between the amine and the oxygen of the amide group, although the electrowithdrawing character of the second group might still be a drawdown for complexation. And **L3**, with the most coordinating available heteroatoms, presents the highest association constant. The sharp decrease in the association constant amog **L4-L6** can be hypothesized by the extra carbon providing a spacer of three carbons between the heteroatoms alongside the benzene moiety that increases rigidity and therefore more constrains for complexation.These results are in agreement with other dansyl derivatives studied previously in our group, being Hg^{2+} or Cu^{2+} the higher values observed.

The acid-base properties of all dansyl derivatives were also evaluated. While consistent results were observed across all compounds, Fig. 4 specifically depicts the behavior of **L1** when treated with HCl and ammonia. Detailed results for the other derivatives are available in the Supplementary Material (Figs. S19–S22). The addition of acid produces a decrease in the absorption at 345 nm, as well as, in the emission intensity at 519 nm. Conversely, when ammonia is added, the opposite is observed with an increase in the absorption band at 345 nm, which is accompanied by a rise, ca. 60% in the emission intensity of **L1**.

Having in mind these results, the acid-base responsive dansyl derivatives were introduced into PMMA polymers offering several applications, such as environmental.

3.4. Low-cost dye doped PMMA polymers: detection of acidic environments

Incorporation of acid-base responsive dansyl derivatives into polymers can transform them into smart, adaptive materials with a broad range of potential applications in sensing, electronics, and healthcare, among others. The creation of a polymer acid-base sensitive to environment can be crucial in applications where pH monitoring or sensing is essential.

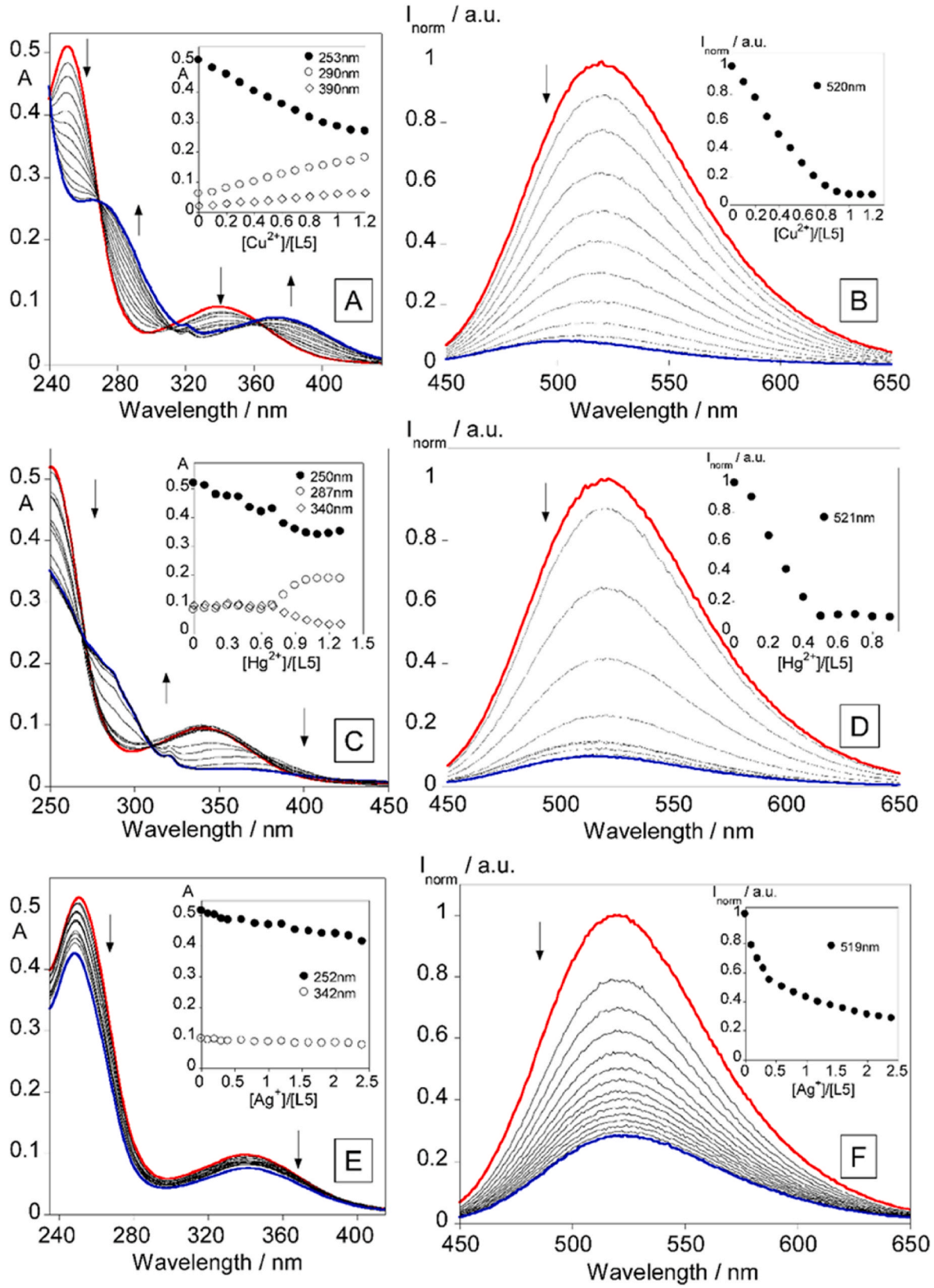

Fig. 3. Spectrophotometric and spectrofluorometric titrations of dansyl derivative **L5** with increased additions of Cu^{2+} (A, B), Hg^{2+} (C, D), and Ag^{+} (E, F) in CH_3CN. The inset represents the absorption (A, C, E) and emission (B, D, F) as a function of $[Cu^{2+}]/[\mathbf{L5}]$, $[Hg^{2+}]/[\mathbf{L5}]$ and $[Ag^{+}]/[\mathbf{L5}]$ respectively. $[\mathbf{L5}] = 20\ \mu M$, $\lambda_{exc\mathbf{L5}} = 337$ nm, $T = 298$ K).

Table 4
Stability association constants and stoichiometry for the complexes formed from **L1** to **L6** with Cu^{2+}, Hg^{2+}, Ag^{+} ions, in CH_3CN.

Compounds (L)	Metal (M)	Association constants ($LogK_{ass.}$)	L:M
L1	Cu^{2+}	7.22 ± 0.06	1:1
	Hg^{2+}	9.10 ± 0.01	1:1
L2	Cu^{2+}	10.54 ± 0.01	1:1
	Hg^{2+}	8.96 ± 0.01	1:1
L3	Cu^{2+}	11.40 ± 0.02	1:1
	Hg^{2+}	9.44 ± 0.01	1:1
L4	Cu^{2+}	5.34 ± 0.01	1:1
	Hg^{2+}	5.76 ± 0.01	1:1
L5	Cu^{2+}	5.92 ± 0.01	1:1
	Hg^{2+}	5.20 ± 0.01	1:1
	Ag^{+}	5.30 ± 0.01	1:1
L6	Cu^{2+}	7.15 ± 0.02	1:1
	Hg^{2+}	5.67 ± 0.01	1:1

PMMA polymers doped with compounds **L1**-**L6** were successfully synthetized. All doped polymers from **L1** to **L6**, except for **L5**, showed to be sensitive to the acid-base environment (see Supplementary Material: Fig. S23). Fig. 5 shows the results obtained for **L1**, as a representative case. As the first approach, the **L1**@PMMA polymer was immersed into a concentrated solution of HCl, and at every 5 minute intervals an emission spectrum was recorded. Afterwards, another polymer was submitted to HCl vapours, and the emission spectra were taken at every 20 min. All doped polymers have all an initial strong blue emission, which was progressively decreasing in both acidic environments. It is interesting to note, that in solution in general all compounds have a green emission, but when incorporated into a PMMA such emission suffers a blue shift, emitting consequently a blue color. As previously seen these compounds are highly influenced by the surrounding solvent molecules, affecting their electronic properties. In a solid polymer matrix, the local environment is different, the polymer is a more rigid structure causing changes in the molecular conformation or restricting the rotational and vibrations of the molecule, affecting the electronic transitions and thus its emission wavelength.

In the second approach, the doped polymers were dipped in a 2–12 M gradient of HCl solutions (Fig. 5C and D; S24). By emission, it is possible to verify the doped polymer response at the lowest HCl concentration 2 M, with a reduction in the emission signal of ca. 25%. Visually under a UV lamp, a result is verified after 4 M, with a total absence of emission at 12 M. The reproducibility of the dye-doped polymers was proved by continuous immersion of the polymers in HCl and ammonia for different cycles (See Supplementary Material: Fig. S25).

4. Conclusions

The synthesis and characterization of six dansyl derivatives have led to the creation of innovative sensing materials when incorporated into PMMA polymers. These compounds exhibited a positive solvatochromic effect, causing a shift in emission colour from yellow to green as solvent polarity increased, accompanied by red-shifts of 30–40 nm in emission maximum wavelength. The studies towards metal ions revealed the sensitivity of these compounds to Cu^{2+} and Hg^{2+}, with complete emission intensity quenching upon the addition of no more than 2

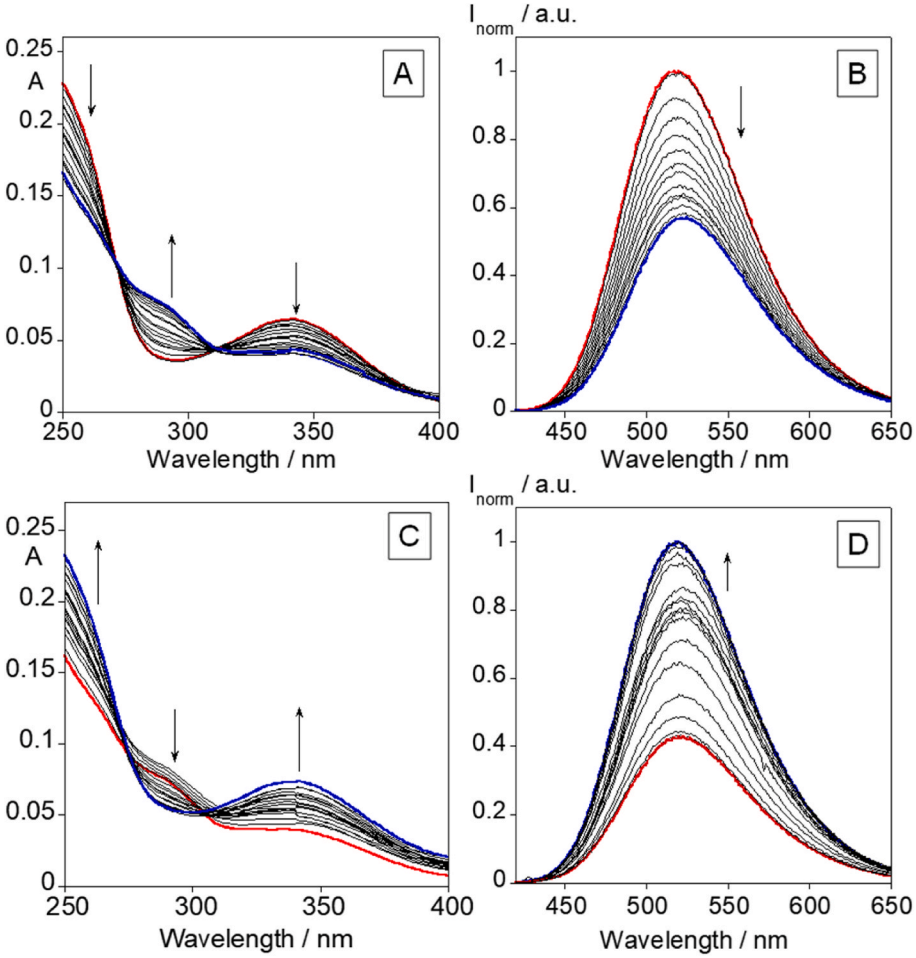

Fig. 4. Spectrophotometric and spectrofluorometric titrations of dansyl derivative **L1** with increased additions of HCl (A, B), and ammonia (C, D) in CH_3CN. [**L1**] = 20 μM, λ_{excL1} = 345 nm, T = 298 K).

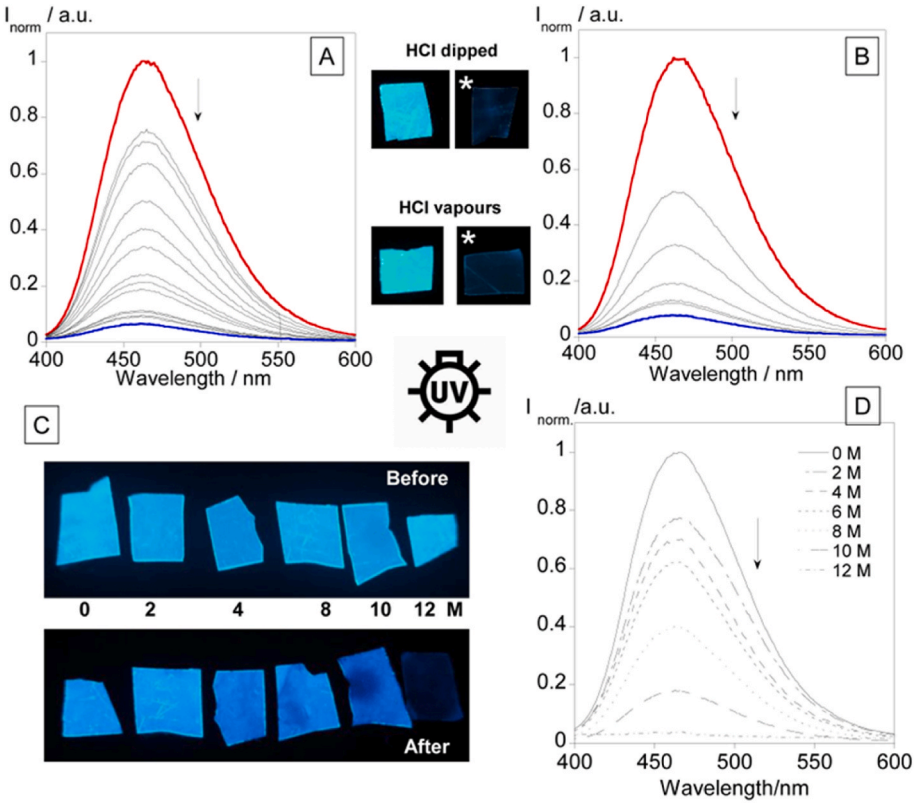

Fig. 5. (A) Emission spectra of successive immersion of **L1** doped PMMA polymer film in a concentrated HCl solution (5 M in 5min). (B) Emission spectra of exposure of **L1** to HCl vapours (20 m in 20 m), T = 298 K. Images under a UV lamp (C) and emission spectra (D) of **L1** immersion in the HCl concentrations from 0 to 12 M, $\lambda_{excL1} = 345$ nm.

equivalents of each metal. The acid-sensing studies conducted showed that all six compounds, except **L3**, hold substantial potential for developing cost-effective systems to detect acidic environments. They displayed significant emission intensity quenching and recovery when titrated with HCl and NH_3, respectively, in solution. In PMMA polymer matrices, gradual intensity reductions were observed after successive immersions in HCl and exposure to HCl vapours, and these systems exhibited good emission intensity reversibility after ten cycles, underscoring their reusability.

Thus, these materials demonstrate a potent combination of solvatochromism, selective metal ion sensing, and acid-base responsiveness. Moreover, this work highlights the compounds' sensitivity to environmental changes, particularly in detecting metal ions and pH variations.

The integration into polymers not only enhances the practical utility of the dansyl derivatives but also opens new avenues for their application in environmental monitoring and bioanalytical chemistry. Future work could explore further functionalization to enhance their sensitivity and selectivity, paving the way for more robust and versatile sensing platforms.

CRediT authorship contribution statement

Gonçalo Pedro: Writing – review & editing, Visualization, Software, Investigation, Formal analysis, Data curation. **Frederico Duarte:** Writing – review & editing, Software, Investigation, Formal analysis, Data curation. **Georgi M. Dobrikov:** Writing – review & editing, Visualization, Validation, Resources, Investigation, Formal analysis. **Atanas Kurutos:** Writing – review & editing, Validation, Investigation, Funding acquisition, Formal analysis, Conceptualization. **Hugo M. Santos:** Writing – review & editing, Visualization, Validation, Software, Investigation. **José Luis Capelo-Martinez:** Writing – review & editing, Visualization, Resources, Funding acquisition. **Elisabete Oliveira:** Writing – review & editing, Writing – original draft, Validation, Supervision, Software, Investigation, Formal analysis, Data curation, Conceptualization. **Carlos Lodeiro:** Writing – review & editing, Writing – original draft, Supervision, Resources, Project administration, Funding acquisition, Formal analysis, Data curation, Conceptualization.

Declaration of competing interest

The authors declare the following financial interests/personal relationships which may be considered as potential competing interests.

Data availability

Data will be made available on request.

Acknowledgements

This work was supported by the Associate Laboratory for Green Chemistry - LAQV which is financed by national funds from FCT/MCTES (LA/P/0008/2020 DOI 10.54499/LA/P/0008/2020, UIDP/50006/2020 DOI 10.54499/UIDP/50006/2020 and UIDB/50006/2020 DOI 10.54499/UIDB/50006/2020) as well as the Scientific Society PROTEOMASS (Portugal) for funding support (General Funding Grant). F.D. thanks FCT/MEC (Portugal) for his doctoral grant 2021.05161.BD. E.O thanks FCT/MEC (Portugal) for the individual contract, CEECIND/05280/2022. HMS acknowledges the Associate Laboratory for Green Chemistry-LAQV (LA/P/0008/2020) funded by FCT/MCTES for his research contract.

The financial support by the Bulgarian National Science Fund (BNSF) under grant – "Novel styryl and polymethine fluorophores as potential theranostic agents "contract KP-06-M59/1 from 15.11.2021 is gratefully

acknowledged by A.K. This work is also developed and acknowledged by A.K. as part of contract BG-RRP-2.004-0002-C01, Laboratory of Organic Functional Materials (Project BiOrgaMCT), Procedure BG-RRP-2.004, Establishing of a network of research higher education institutions in Bulgaria", funded by BULGARIAN NATIONAL RECOVERY AND RESILIENCE PLAN". G.D. thanks to the European Regional Development Fund within the Operational Programme Science and Education for Smart Growth 2014–2020 under the Project Center of Exellence: National center of mechatronics and clean technologies - BG05M2OP001-1.001-0008 for the financial support.

Appendix A. Supplementary data

Supplementary data to this article can be found online at https://doi.org/10.1016/j.dyepig.2024.112042.

References

[1] Sivaraman G, Iniya M, Anand T, Kotla NG, Sunnapu O, Singaravadivel S, et al. Chemically diverse small molecule fluorescent chemosensors for copper ion. Coord Chem Rev 2018;357:50–104. https://doi.org/10.1016/j.ccr.2017.11.020.
[2] Oliveira E, Bértolo E, Núñez C, Pilla V, Santos HM, Fernández-Lodeiro J, et al. Front cover: green and red fluorescent dyes for translational applications in imaging and sensing analytes: a dual-color flag (ChemistryOpen 1/2018). ChemistryOpen 2018;7. https://doi.org/10.1002/open.201700167. 1–1.
[3] Murov SL, Carmichael I, Hug GL. Handbook of photochemistry. second ed. CRC Press; 1993.
[4] Li Y-H, Chan L-M, Tyer L, Moody RT, Himel CM, Hercules DM. Solvent effects on the fluorescence of 1-(dimethylamino)-5-naphthalenesulfonic acid and related compounds. J Am Chem Soc 1975;97:3118–26. https://doi.org/10.1021/ja00844a033.
[5] Qin X, Yang X, Du L, Li M. Polarity-based fluorescence probes: properties and applications. RSC Med Chem 2021;12:1826–38. https://doi.org/10.1039/D1MD00170A.
[6] Wei P, Xiao L, Gou Y, He F, Zhou D, Liu Y, et al. Fluorescent "on–off–on" probe based on copper peptide backbone for specific detection of Cu(II) and hydrogen sulfide and its applications in cell imaging, real water samples and test strips. Microchem J 2022;182:107848. https://doi.org/10.1016/j.microc.2022.107848.
[7] Duarte F, Dobrikov G, Kurutos A, Santos HM, Fernández-Lodeiro J, Capelo-Martinez JL, et al. Enhancing water sensing via aggregation-induced emission (AIE) and solvatofluorochromic studies using two new dansyl derivatives containing a disulfide bound: pollutant metal ions detection and preparation of water-soluble fluorescent polymeric particles. Dyes Pigments 2023;218:111428. https://doi.org/10.1016/j.dyepig.2023.111428.
[8] Duarte F, Dobrikov G, Kurutos A, Capelo-Martinez JL, Santos HM, Oliveira E, et al. Development of fluorochromic polymer doped materials as platforms for temperature sensing using three dansyl derivatives bearing a sulfur bridge. J Photochem Photobiol Chem 2023;445:115033. https://doi.org/10.1016/j.jphotochem.2023.115033.
[9] Métivier R, Leray I, Lebeau B, Valeur B. A mesoporous silica functionalized by a covalently bound calixarene-based fluoroionophore for selective optical sensing of mercury(ii) in water. J Mater Chem 2005;15:2965. https://doi.org/10.1039/b501897h.
[10] Algethami JS. A review on recent progress in organic fluorimetric and colorimetric chemosensors for the detection of $Cr^{3+/6+}$ ions. Crit Rev Anal Chem 2022:1–21. https://doi.org/10.1080/10408347.2022.2082242.
[11] Zhou M, Wang X, Huang K, Huang Y, Hu S, Zeng W. A fast, highly selective and sensitive dansyl-based fluorescent sensor for copper (II) ions and its imaging application in living cells. Tetrahedron Lett 2017;58:991–4. https://doi.org/10.1016/j.tetlet.2017.01.090.
[12] Li Y, Ren Z, Ge Y, Di C, Zhou J, Wu J, et al. A novel peptide fluorescent probe based on different fluorescence responses for detection of mercury species and hydrogen sulfide. Microchem J 2023;184:108160. https://doi.org/10.1016/j.microc.2022.108160.
[13] Stuart MAC, Huck WTS, Genzer J, Müller M, Ober C, Stamm M, et al. Emerging applications of stimuli-responsive polymer materials. Nat Mater 2010;9:101–13. https://doi.org/10.1038/nmat2614.
[14] Adhikari B, Majumdar S. Polymers in sensor applications. Prog Polym Sci 2004;29:699–766. https://doi.org/10.1016/j.progpolymsci.2004.03.002.
[15] Galhano J, Marcelo GA, Kurutos A, Bértolo E, Capelo-Martinez JL, Lodeiro C, et al. Development of low-cost colourimetric and pH sensors based on PMMA@Cyanine polymers. Dyes Pigments 2022;200:110154. https://doi.org/10.1016/j.dyepig.2022.110154.
[16] Cheng H, Song F-Q, Zhao N-N, Song X-Q. A hydrostable Zn^{2+} coordination polymer for multifunctional detection of inorganic and organic contaminants in water. Dalton Trans 2021;50:16110–21. https://doi.org/10.1039/D1DT03022A.
[17] Gayathri P, Moon D, Anthony SP. Rewritable fluorescent platform and reusable hydrazine sensing thin film using aldehyde functionalized fluorophore integrated PMMA polymer matrix. Mater Chem Phys 2019;235:121753. https://doi.org/10.1016/j.matchemphys.2019.121753.
[18] Jiménez R, Duarte F, Nuti S, Campo JA, Lodeiro C, Cano M, et al. Thermochromic and acidochromic properties of polymer films doped with pyridyl-β-diketonate boron(III) complexes. Dyes Pigments 2020;177:108272. https://doi.org/10.1016/j.dyepig.2020.108272.
[19] Song F-Q, Cheng H, Zhao N-N, Song X-Q. Construction of enhanced fluorescence sensors in aqueous media by cation regulation and hybridization. J Lumin 2021;239:118338. https://doi.org/10.1016/j.jlumin.2021.118338.
[20] Gülle S, Çelik Erbaş S. A selective fluorescence sensor for Fe (III) based on phenanthroimidazole imine compound. J Fluoresc 2018;28:445–51. https://doi.org/10.1007/s10895-017-2207-y.
[21] Mironenko AY, Sergeev AA, Nazirov AE, Leonov AA, Bratskaya SY, Voznesenskiy SS. Sensitive coatings for luminescence detection of Cu(II) in solutions. Solid State Phenom 2015;245:243–6. https://doi.org/10.4028/www.scientific.net/SSP.245.243.
[22] Gans P, Sabatini A, Vacca A. Investigation of equilibria in solution. Determination of equilibrium constants with the HYPERQUAD suite of programs. Talanta 1996;43:1739–53. https://doi.org/10.1016/0039-9140(96)01958-3.
[23] Berlman IB, Berlman IB, Berlman IB. Handbook of fluorescence spectra of aromatic molecules. second ed. New York: Academic Press, NY; 1971.
[24] Montalti M, Credi A, Prodi L, Gandolfi MT. Handbook of photochemistry. third ed. BOCA: Taylor & Francis, Boca Raton; 2006.
[25] Shi F, Tse MK, Zhou S, Pohl M-M, Radnik J, Hübner S, et al. Green and efficient synthesis of sulfonamides catalyzed by nano-Ru/Fe_3O_4. J Am Chem Soc 2009;131:1775–9. https://doi.org/10.1021/ja807681v.
[26] Yang Y, Yu X, He N, Huang X, Song X, Chen J, et al. $FeCl_3$ -catalyzed oxidative amidation of benzylic C–H bonds enabled by a photogenerated chlorine-radical. Chem Commun 2023;59:10299–302. https://doi.org/10.1039/D3CC03186A.
[27] Huang F-Q, Dong X, Qi L-W, Zhang B. Visible-light photocatalytic α-amino C(sp3)–H activation through radical translocation: a novel and metal-free approach to α-alkoxybenzamides. Tetrahedron Lett 2016;57:1600–4. https://doi.org/10.1016/j.tetlet.2016.02.108.
[28] Ye W, Liu Y, Ren Q, Liao T, Chen Y, Chen D, et al. Design, synthesis and biological evaluation of novel triazoloquinazolinone and imidazoquinazolinone derivatives as allosteric inhibitors of SHP2 phosphatase. J Enzym Inhib Med Chem 2022;37:1495–513. https://doi.org/10.1080/14756366.2022.2078968.
[29] Tang B-D, Zhang J-Y, Ma H-X, Wang N, An X, Li G-M, et al. SYNTHESIS, CRYSTAL STRUCTURE, AND DFT STUDY OF 1-(PYRROLIDIN-1- YL-METHYL)-4-(THIOPHEN-2-YL-METHYL)- [1,2,4]TRIAZOLO[4,3-a]QUINAZOLIN-5(4H)-ONE. J Struct Chem 2022;63:19–25. https://doi.org/10.1134/S0022476622010036.
[30] Zaytsev VP, Revutskaya EL, Kuźmenko MG, Novikov RA, Zubkov FI, Sorokina EA, et al. Synthesis of furyl-, furylvinyl-, thienyl-, pyrrolinylquinazolines and isoindolo[2,1-a]quinazolines. Russ Chem Bull 2015;64:1345–53. https://doi.org/10.1007/s11172-015-1016-1.
[31] Jang Y, Lee SB, Hong J, Chun S, Lee J, Hong S. Synthesis of 2-aryl quinazolinones *via* iron-catalyzed cross-dehydrogenative coupling (CDC) between N–H and C–H bonds. Org Biomol Chem 2020;18:5435–41. https://doi.org/10.1039/D0OB00866D.
[32] Sanmartín-Matalobos J, Bermejo-Barrera P, Pérez-Juste I, Fondo M, García-Deibe AM, Alves-Iglesias Y. Experimental and computational studies on the interaction of a dansyl-based fluorescent schiff base ligand with Cu2+ ions and CuO NPs. Int J Mol Sci 2022;23:11565. https://doi.org/10.3390/ijms231911565.
[33] Ambati NB, Anand V, Hanumanthu P. A facile synthesis of 2-N(methyl amino) benzothiazoles. Synth Commun 1997;27:1487–93. https://doi.org/10.1080/00397919708006084.
[34] Aliaga-Alcalde N, Rodríguez L. Solvatochromic studies of a novel Cd2+– anthracene-based curcuminoid and related complexes. Inorg Chim Acta 2012;380:187–93. https://doi.org/10.1016/j.ica.2011.08.052.
[35] Oliveira E, Baptista RMF, Costa SPG, Raposo MMM, Lodeiro C. Synthesis and solvatochromism studies of novel bis(indolyl)methanes bearing functionalized arylthiophene groups as new colored materials. Photochem Photobiol Sci 2014;13:492–8. https://doi.org/10.1039/c3pp50352f.
[36] Marcelo GA, Pires SMG, Faustino MAF, Simões MMQ, Neves MGPMS, Santos HM, et al. New dual colorimetric/fluorimetric probes for Hg2+ detection & extraction based on mesoporous SBA-16 nanoparticles containing porphyrin or rhodamine chromophores. Dyes Pigments 2019;161:427–37. https://doi.org/10.1016/j.dyepig.2018.09.068.
[37] Gonc AC, Luis J, Lodeiro C, Dos AA. Sensors and Actuators B : chemical A seleno-pyrene selective probe for Hg 2 + detection in either aqueous or aprotic systems, vol. 239; 2017. p. 311–8. https://doi.org/10.1016/j.snb.2016.08.014.
[38] Pinheiro D, De Castro CS, Seixas De Melo JS, Oliveira E, Nuñez C, Fernández-Lodeiro A, et al. From yellow to pink using a fluorimetric and colorimetric pyrene derivative and mercury (II) ions. Dyes Pigments 2014;110:152–8. https://doi.org/10.1016/j.dyepig.2014.04.012.